

Design and Failure Analysis of SAE-9254 Helical Suspension Spring



Prince Raj Krishna, Sameer Panwar, Pratham Purkait, Prateek Jha, and Sushila Rani

Abstract Helical suspension spring is used for automotive suspension in vehicles because of its high fatigue, sag resistance, high strength and toughness with fine grain structure. If the suspension spring is failed in service, it results in severe accidents, economic and time loss. The causes of helical suspension spring failure have been mentioned in the literature. The main causes of its premature failure are raw material defects, surface wear, non-metallic inclusions, improper heat treatment and decarburization. In this research work, a helical suspension spring has been designed, which is failed during manufacturing at coiling stage. The real case failed helical suspension spring has been analysed experimentally and computationally to find root causes of its failure. Through experimental results, it is concluded that the spring has been failed due to formation of transverse crack on its cross section. Martensite and bainite was also formed due to variation in surface and core hardness. Decarburization and skin hardness on the outer periphery of spring coil also play a role in the helical suspension spring's catastrophic failure. From the computational results, it is observed that at the point of surface wear there is high stress concentration region. The difference found in stresses at the point of surface wear and spring material results in failure of helical suspension spring.

Keywords Helical suspension spring · Scanning electron microscope (SEM) · Transverse cracks · Von-Mises stress

P. R. Krishna (✉) · S. Panwar · P. Purkait · P. Jha · S. Rani
Department of Mechanical Engineering, Delhi Technological University, Delhi, India
e-mail: 221prk@gmail.com

S. Panwar
e-mail: smrpanwar26@gmail.com

P. Purkait
e-mail: pratham29112000@gmail.com

P. Jha
e-mail: prateekjha99@gmail.com

S. Rani
e-mail: sushilarani@dtu.ac.in

1 Introduction

Helical springs are an energy-efficient device that offers resistance to compressive and tensile loads. It is generally made up of steel wires in the form of helix to absorb and eject energy between the surfaces, thus allowing it to regain its original shape despite significant deflection [1]. The manufacturing of the helical suspension spring begins with cold winding of the heat-treated, tempered and coated steel wires. The coiling of such high strength steel wire is a critical process as it brings a premature failure like raw material imperfections, non-metallic inclusions, inappropriate heat treatment and decarburization [2].

Ke et al. [3] have compared different composite materials for the designing of helical spring on the basis of mechanical properties and production cost. They have evaluated mechanical properties of composite materials experimentally as well as computationally. They came to the conclusion that combined use of carbon and glass fibre is the best material for building composite springs. The ideal ply angle for the composite helical spring is also recommended to be $\pm 45^\circ$. Prawoto et al. [4] have studied different types of defects occurred in helical springs that leads to its failure. They have analysed raw material flaws including high inclusion concentrations, manufacturing flaws such delayed quench cracking, failures caused by complex stress and chemically generated failures. They have concluded that the regions for high stress concentration cause fatigue failure of springs. Aniekan et al. [5] have conducted a comparative study of three different materials, i.e. high carbon steel, stainless steel and chrome vanadium steel for designing of helical compression spring. The designed load is taken as vehicle's curb weight. Because of the other alloying components and the high chromium content, they concluded that when loading parameters increases, high carbon steel will be the first material to fail in the time of operation, but stainless steel and chrome vanadium may show a continuous degree of durability before fracture. Further, it is also concluded that failure of spring caused by implicit imperfections in the raw material such as inappropriate heat treatment, decarburization, inclusions, surface flaws due to insignificant shot-peening. Das et al. [6] have investigated helical spring which is failed at the coiling stage to investigate the root causes of breakage of spring during production and also its quality aspect. They have observed that spring breakage was caused by phosphorous and chromium segregation in the form of martensitic billet. This causes increased stress levels, which leads to the formation of internal cracks and spring wire breaking. They have recommend that the wire drawing process should be enhanced, including greater lubrication and taper drafting to prevent abrasion on the drawn wire surface. Fragoudakis et al. [7] have studied and explored the methods for increasing the hardness of spring wire. They have heat-treated 56SiCr7 steel to increase its surface hardness and fatigue resistance. Experiments have been performed to measure the thickness of the decarb layer, core hardness, and surface hardness of the heat-treated steel. They have concluded that the core hardness of heat-treated steel has increased but its surface hardness reduces due to decarburization. Also, after heat treatment

steel is shot-peened to induce compressive residual stresses on the steel's surface, which increases its fatigue life.

Puff et al. [8] have studied the effects of non-metallic inclusions which are responsible for an early break down of a helical spring made up of VDSiCr spring steel. The residual stresses developed around the inclusion due to shot-peening are evaluated computationally. The three-dimensional CAD model of helical spring is created and analysed using finite element-based software ANSYS®. The analysis shows the stress concentration around the inclusion and hence validates the results. These stress concentration regions led to the failure of spring. Suzuki et al. [9] have analysed and evaluated the effects of Si and Cr concentrations on the bainite microstructure of medium carbon steels. Four different medium carbon steels were compared after being austenitized at 1000 °C. The microstructures observed through Scanning electron microscopy and transmission electron microscopy revealed slower bainite transformation kinetics when Si and Cr content were increased. It was also observed that the hardness decreases due to bainite formation which reduces the martensite after heat treatment. Pilar et al. [10] collected a spring of an actuator drive that failed under torsion. Various metallographic and fractographic analysis of the fractured surface revealed that the main cause of failure is a poor surface finish which results in improper surface roughness and ultimately leads to crack propagation which results in fracture of spring.

Pastorcic et al. [11] have performed fatigue analysis of a real case failed coil spring removed from a passenger vehicle. They have observed the formation of corrosion pits due to continuous contact between the coils experimentally. They have concluded that these corrosion pits served as regions of crack initiation, which propagate further on loading and resulted in catastrophic failure of coil spring. Vukelic et al. [12] have analysed a failed coil spring of a motor vehicle to find its root causes of failure. Visual observation of the broken surface, chemical composition analysis with the help of a glow discharge spectrometer, hardness testing, optical and scanning electron microscopy analysis of the failed surface were all used to analyse the failed spring experimentally. They came to the conclusion that the wire's protective paint coating was destroyed, causing corrosion pits to form. These pits acted as crack initiation points, resulting in fatigue failure of coil spring due to corrosion. Das et al. [13] have carried out an investigation on the prematurely failed coil suspension spring of a car. Visual examination, microstructural analysis, scanning electron microscopy (SEM), inclusion percentage by optical microscopy, hardness testing, residual stress evaluation by X-ray diffraction (XRD), and instrumental chemical analysis were used to investigate the failed suspension spring. They came to the conclusion that due to the insufficient shot-peening and the presence of excess oxide presence in the steel, a premature failure in spring was occurred.

Sreenivasan et al. [14] have analysed and evaluated the performance of a motorcycle's coil spring suspension system constructed of several fibre materials. The three-dimensional CAD model of the suspension system was created and analysed using finite element-based software ANSYS® 16.0. They have found that the E-Glass fibre was subjected to very low stress, strain and more safer material as compared to other materials such as carbon fibre or Kevlar. Yan et al. [15] have analysed a

real case failed automobile coil spring of ASTM 9260 spring steel to determine the causes of its premature failure. The failed spring was examined experimentally using various techniques include visual observation, optical microscope, scanning electron microscope (SEM), energy dispersive spectrometer (EDS) analysis. On the surface of the failing spring, they discovered extensive wear marks and machinery indentations, indicating a defective installation that could cause excessive strains when subjected to service loads. They have concluded that radiating ridges coming from the indentation tip served as the crack initiation point. An increase in the load results in crack propagation which leads to catastrophic failure of automobile coil spring. Stephen et al. [16] have performed computational analysis using ANSYS® software to compare three chosen materials namely, Structural steel, S-Glass Epoxy composite and Epoxy-Carbon prepreg composite to find the applicability of suspension springs in automobile. They have found that the stiffness and deflections calculated using simulation and theoretical models for all the chosen materials were nearly same, with a variation of around 5%. They have concluded that composites are much better in terms of weight and strength. However, composite springs have a lesser load carrying capacity than steel springs.

In this research work, a helical spring is designed which is failed during its manufacturing at coiling stage. This failed spring is further analysed experimentally and computationally to find its root causes of failure. The computational analysis of failed spring is performed to find out the regions of maximum stresses at which failure takes place. Visual observations, chemical composition analysis of material, scanning electron microscopy (SEM) and energy dispersive spectroscopy (EDS) are the experimental techniques used in this research work. During the inspection of the failed spring, it was revealed that the spring was failed as a result of a combination of decarburization, hardness variations and the development of bainite and martensite.

2 Design of Helical Suspension Spring

High fatigue strength, ductility, resilience and creep resistance are all requirements for the material used in spring design. In this research work, the material selected to design helical suspension spring for motorbike is SAE-9254 as it provides fatigue resistance, toughness and resistance to shock, vibration and variable loading. The various material properties of SAE-9254 are tabulated in Table 1. Following data has been used for the design calculations of springs.

Axial load, W is assumed to be 1500 N.

Table 1 Various material properties of SAE-9254

Material	Modulus of rigidity, (G)	External diameter of coil spring, (D_o)	Internal diameter of coil spring, (D_i)	Pitch, (P)
SAE-9254	72 GPa	70 mm	45 mm	35 mm

The mass of the system to be analysed is assumed as follows:

Mass of the bike = 125 kg.

Mass of one person = 65 kg.

Mass of two person = 130 kg.

Mass of bike + two persons = 255 kg.

Out of total mass 60% mass is on the rear suspension = 153 kg.

Dynamic mass and rear suspension = $2 \times 153 = 306$ kg.

The mass on 1 shock absorber = $\frac{306}{2} = 153$ kg.

Load on 1 shock absorber = $153 \times 9.8 = 1499.4 \sim 1500$ N.

No. of active coils, $n = 5$.

Equations (1) and (2) represent the relationship between external diameter of coil (D_o), internal diameter of coil (D_i), mean diameter of coil (D), wire diameter (d). From the relations (1) and (2), D and d can be calculated.

$$D_o = D + d \quad (1)$$

$$D_i = D - d \quad (2)$$

From Eqs. (1) and (2), the values of mean diameter of coil (D) and diameter of spring wire (d) are evaluated as 57.5 mm and 12.5 mm, respectively.

The Torsional shear stress, τ_1 is calculated from Eq. (3)

$$\tau_1 = \frac{8WD}{\pi d^3} \quad (3)$$

From Eq. (3), the value of torsional shear stress (τ_1) is evaluated as 112.5 MPa.

Direct shear stress, τ_2 is evaluated from Eq. (4)

$$\tau_2 = \frac{4W}{\pi d^2} \quad (4)$$

From Eq. (4), the value of direct shear stress (τ_2) is calculated as 12.23 MPa.

Resultant shear stress induced for inner edge of wire, τ is calculated from Eq. (5).

(a) For inner edge of wire

$$\begin{aligned} \tau &= \tau_1 + \tau_2 \\ \tau &= \frac{8WD}{\pi d^3} + \frac{4W}{\pi d^2} \end{aligned} \quad (5)$$

From Eq. (5), the value of Resultant shear stress induced (τ) is evaluated as 124.73 MPa.

Resultant shear stress induced for outer edge of wire, τ is calculated from Eq. (6)

(b) For outer edge of wire

$$\begin{aligned}\tau &= \tau_1 - \tau_2 \\ \tau &= \frac{8WD}{\pi d^3} - \frac{4W}{\pi d^2}\end{aligned}\quad (6)$$

From Eq. (6), the value of Resultant shear stress induced (τ) is evaluated as 100.27 MPa.

Wahl's Correction factor, K_w is calculated from Eq. (7)

$$K_w = \frac{4C - 1}{4C - 4} + \frac{0.615}{C}.\quad (7)$$

Spring index, C is calculated from Eq. (8)

$$C = \frac{D}{d}\quad (8)$$

From Eq. (7), the value of Wahl's Correction factor (K_w) is evaluated as 1.341.

From Eq. (8), the value of spring index (C) is evaluated as 4.6.

The Maximum shear stress, τ_{\max} is calculated from Eq. (9)

$$\tau_{\max} = K_w \frac{8WD}{\pi d^3}\quad (9)$$

From Eq. (9), the value of Maximum shear stress (τ_{\max}) is evaluated as 151 MPa.

The Angular deflection of helical spring, θ is calculated from Eq. (10)

$$\theta = \frac{16WD^2n}{Gd^4}\quad (10)$$

From Eq. (10), the value of Angular deflection of helical spring (θ) is calculated as 0.226 radians.

The strain energy of helical spring, U is calculated using Eq. (12)

$$U = \frac{1}{2}T\theta\quad (11)$$

$$U = \frac{1}{2} W = \frac{D}{2}\theta\quad (12)$$

From Eq. (12), the value of Strain energy of helical spring (U) is evaluated as 4873.125 kJ.

The Axial deflection of spring, δ is evaluated using Eq. (13)

$$\delta = \frac{8WD^3n}{Gd^4}\quad (13)$$

From Eq. (13), the value of axial deflection of spring (δ) is calculated as 6.489 mm.

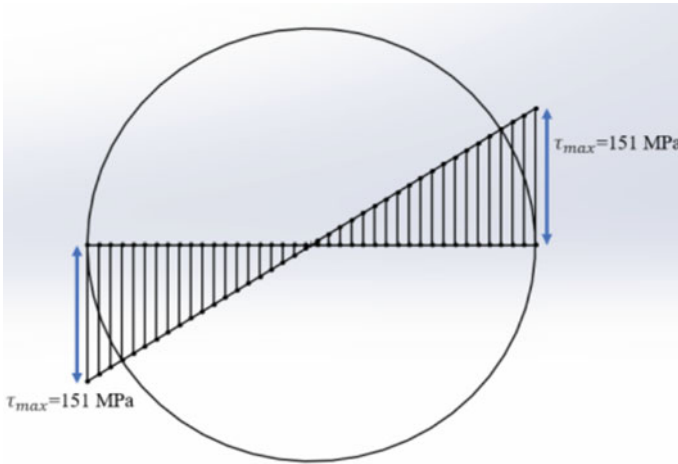


Fig. 1 Shear stress distribution in helical spring

The spring rate or stiffness of spring, K is calculated from Eq. (14)

$$K = \frac{W}{\delta} = \frac{Gd^4}{8D^3n} \quad (14)$$

From Eq. (14), the value of spring rate or stiffness of spring (K) is evaluated as 4.02 N/mm.

The shear stress distribution diagram of helical spring is shown in Fig. 1. In this diagram, the shear stress at the centre is zero but as we move from centre towards the upper fibre and bottom fibre, shear stress varies linearly and reaches a maximum value of 151 MPa. The load deflection diagram is depicted in Fig. 2. In this figure, load varies linearly with deflection as load increases, deflection also increases. All the parameters of designed helical spring are tabulated in Table 2.

3 Manufacturing of Helical Spring

The spring manufacturing is a step-by-step process, which starts with the coiling operation, which is done in two ways—cold coil forming and hot coil forming. In cold coil forming operation, the room temperature is the key requirement for coiling. The hot coiling operation is generally used for very hard or thick wires in which the wire is pre-heated so that the wire becomes sufficiently flexible for coiling. In both the methods, the wire is fed with the help of feed rollers to wind around the guide shaft. Also, the forming rollers, cover plate and shape plate provide support to the wire during coiling (Fig. 3) [2].

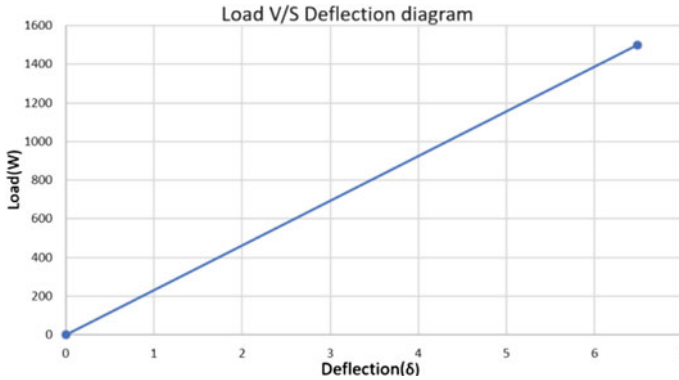


Fig. 2 Rate of change of load with deflection in helical spring

Table 2 Parameters of helical spring

Parameters	Values
External diameter of coil spring (D_o)	70 mm
Internal diameter of coil spring (D_i)	45 mm
Pitch of spring (P)	35 mm
Axial load (W)	1500 N
No of active coils (n)	5
Mean coil diameter of spring (D)	57.5 mm
Spring wire diameter (d)	12.5 mm
Torsional shear stress (τ_1)	112.5 MPa
Direct shear stress (τ_2)	12.23 MPa
Resultant shear stress for inner edge of wire (τ)	124.73 MPa
Resultant shear stress for outer edge of wire (τ)	100.27 MPa
Spring index (C)	4.6
Wahl's correction factor (K_w)	1.341
Maximum shear stress (τ_{max})	151 MPa
Angular deflection of helical spring (θ)	0.226 rad
Strain energy (U)	4873.125 kJ
Axial deflection (δ)	6.489 mm
Spring rate or stiffness of spring (K)	4.02 N/mm

After coiling, tempering is done on spring at a fixed temperature in order to increase the hardness and relieve the internal residual stresses which are setup during coiling operation. Further, tempered spring coil is shot-peened to introduce compressive residual stress in the spring and then this spring coil is coated either by chromium, zinc or liquid plastic, this plating prevent corrosion in the spring.

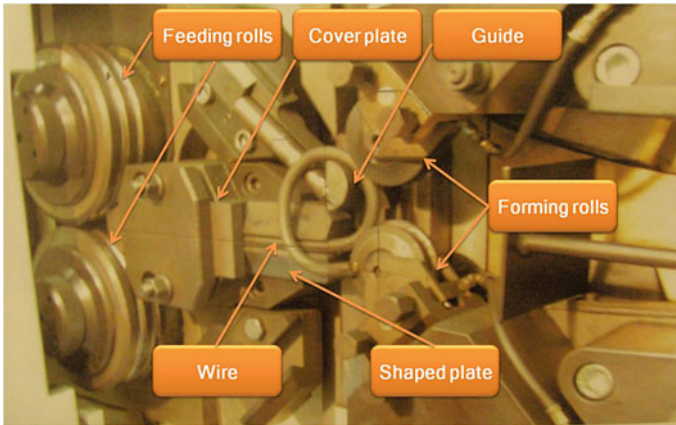


Fig. 3 Coil forming machine. *Source* FEM analysis of the forming process of automotive suspension springs, *Semantic Scholar*

In this research work, during manufacturing of helical suspension spring, the spring wire is broken at the coiling stage. This real case failed high strength SAE-9254 spring wire is analysed experimentally and computationally to find its root causes of failure. The experimental analysis includes visual observations, chemical composition analysis of material, scanning electron microscopy (SEM) and energy dispersive spectroscopy (EDS). The computational analysis of spring wire is performed on a finite element-based software, i.e. ANSYS® to find out the maximum stress regions at which failure takes place.

4 Failure Investigation of High Strength SAE-9254 Spring Wire

4.1 Experimental Procedure

A real case failed helical suspension spring made up of silicon chromium based high strength steel grade SAE-9254 is analysed experimentally to determine the root causes of its failure. A specimen of about 12.5 mm diameter and 20 mm height is cut from the fractured end of the coil by wire cutting process. Further, the specimen was finely polished on Standard Disc Polisher machine (Fig. 4) and etched with 3% nital solution (3 mL HNO₃ in 97 mL ethyl alcohol) [6]. To determine the chemical composition of material of failed spring, AmeCare X-ray energy dispersive spectrometer (EDS) is used to for testing as shown in Fig. 5. The microstructure of the failed spring specimen and its fractured surface morphology are investigated using Metzer METZ 56 monocular inclined metallurgical microscope (Fig. 6).

Fig. 4 Standard disc polisher



Fig. 5 AmeCare XRD (EDS)



Fig. 6 Metzer METZ 56 metallurgical microscope



4.2 Computational Analysis

A three-dimensional CAD model for spring coil forming mechanism was created using SolidWorks. Then this CAD model is imported and analysed in ANSYS® software. Since, the CAD model consists of 9 bodies (Fig. 7) and hence, a patch conforming method was used to create tetrahedron mesh of 3 mm element size as shown in Fig. 8. The finite element model included 53,665 nodes and 28,745 elements. The material selected for spring wire is SAE-9254 and grey cast iron is selected for other bodies. The material properties of SAE-9254 and grey cast iron are tabulated in Tables 3 and 4. The boundary conditions for static analysis of spring coil forming setup are shown in Fig. 9.

The wire was feed to the forming machine by a displacement of 5 cm per second along y-axis with the help of a press. The feed roller, shaped and cover plate were used as support to facilitate the motion of wire only in y-direction. The guide and forming roller helped in the formation of helical coils by bending of wire. Different friction factors are considered between the contact surface of wire and other components of the forming machine to allow proper coil formation, as shown in Table 5 [2]. Static analysis of the spring coil forming mechanism is carried out using ANSYS® software.

5 Results and Discussion

5.1 Visual Examination

The real case failed helical suspension spring made up of high strength steel SAE-9254 is shown in Fig. 10. On visual examination, it is found that there are longitudinal cracks at the outer periphery of spring coil as shown in Fig. 11. Figure 12 depicts

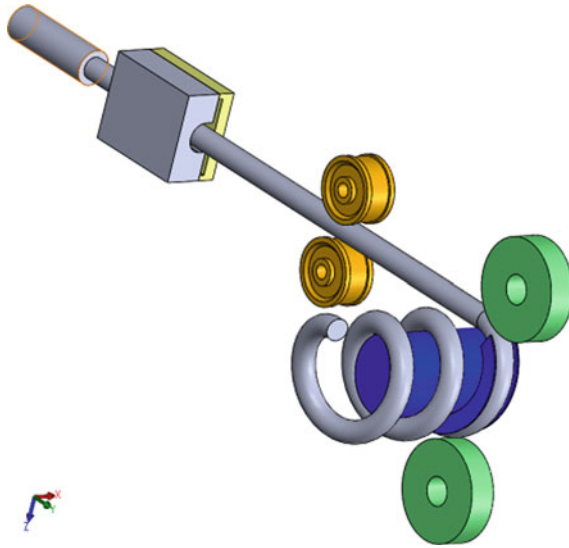


Fig. 7 CAD model of spring coil forming mechanism

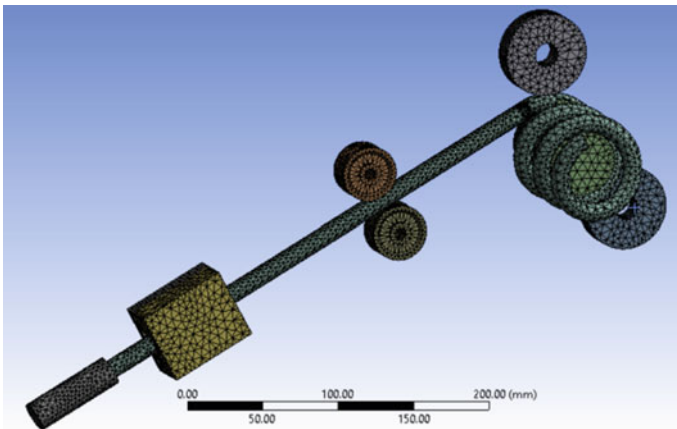


Fig. 8 Mesh model of spring coil forming setup

dark black spots and pits on the cross section of the spring coil. These pits provide the regions of high stress concentration which serve as a notch for crack initiation.

Table 3 Material properties of SAE-9254

SAE-9254	
Density	$7.7 \times 10^{-6} \text{ kg/mm}^3$
Young's modulus	210 GPa
Poisson's ratio	0.3
Bulk modulus	175,000 MPa
Shear modulus	80,769 MPa
Ultimate tensile strength	1704 MPa
Yield strength	1500 MPa

Table 4 Material properties of grey cast iron

Grey cast iron	
Density	$7.2 \times 10^{-6} \text{ kg/mm}^3$
Young's modulus	110 GPa
Poisson's ratio	0.28
Bulk modulus	83,333 MPa
Shear modulus	42,969 MPa
Ultimate tensile strength	240 MPa
Yield strength	0 MPa

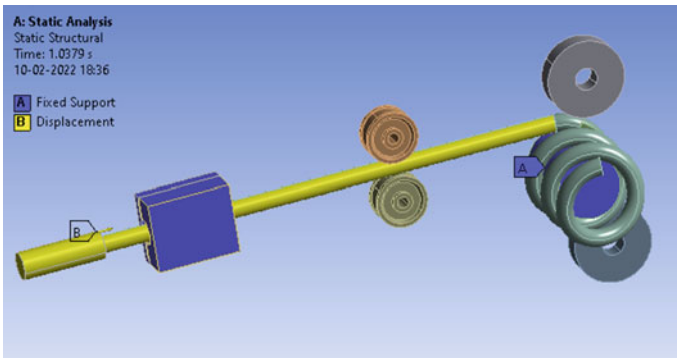


Fig. 9 Boundary conditions for static analysis

5.2 Chemical Analysis of Materials

The chemical composition (%wt) analysis of failed helical suspension spring and the spring wire material SAE-9254 is tabulated in Table 6. The result shows that the failed helical suspension spring material is in accordance with the spring wire material (SAE-9254) but the compositions of elements C, Si, Mn, S, Cr and P are

Table 5 Friction factor between the contact surface of the wire and other part of the coil forming machine

Geometry name	Min	Max
Shaped plate	0.05	0.15
Cover plate	0.05	0.15
Guide	0.05	0.15
Feed roller	0.05	0.15
Forming roller	0.05	0.15

**Fig. 10** Failed helical suspension spring

changed. The %wt of elements Mn, C, Cr is decreased whilst the %wt of elements Si, S and P is increased and the %wt of Ni, Cu and Mo remains unchanged.

Decarburization results in decrease of %wt of carbon which occur due to improper heat treatment conditions. The chemical composition of phosphorus content increases, this brings brittleness in the spring coil due to the segregation of phosphorus on the grain boundaries. During the coiling process, Chromium segregates in the form of martensite billets which results decrease in its %wt as observed in the failed spring. Silicon is used in the formation of inclusion like silicates which stabilize the microstructure during tempering of steel. Manganese also helps in the formation of martensite structure, the manganese present in Manganese Sulphide (MnS) is utilized in the formation of martensite and hence results decrease in %wt of Manganese and increase in %wt of Sulphur.

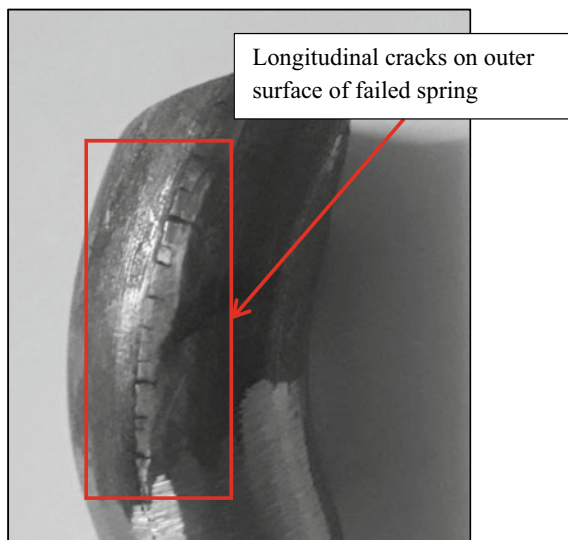


Fig. 11 Longitudinal cracks on outer surface of failed spring

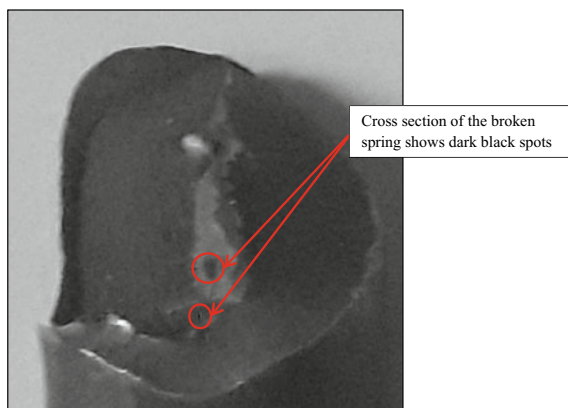


Fig. 12 Cross section of the broken spring shows dark black spots

Table 6 The chemical composition of failed spring and SAE-9254 wire (%wt)

Alloy	C	Si	Mn	Cr	Ni	Mo	S	P	Cu
SAE-9254 (Spring wire)	0.595	1.35	0.706	0.760	< 0.003	0.0049	0.0090	0.0179	< 0.001
Failed spring	0.592	1.36	0.701	0.752	< 0.003	0.0049	0.0094	0.0214	< 0.001

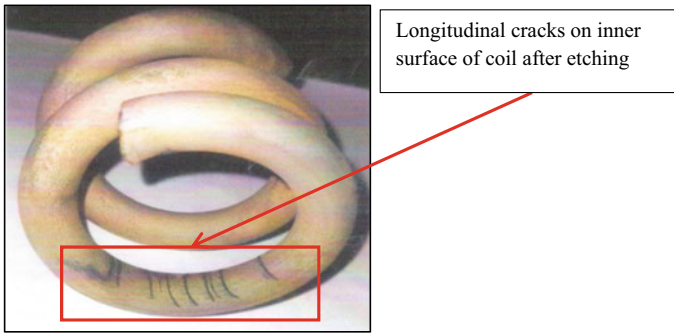


Fig. 13 Longitudinal cracks on inner surface of coil after etching

5.3 Macrostructure Evaluation

The failed helical suspension spring is etched with 3% nital solution (3 mL HNO₃ in 97 mL ethyl alcohol) for 1 h duration (Fig. 13), which removed the phosphate layer from coil and revealed multiple longitudinal cracks on the inner periphery of the spring. Further, on examination of outer periphery, skin hardness is found with decarburization that leads to the formation of internal crack during coil forming operation.

5.4 Microstructure Evaluation

A specimen of about 12.5 mm diameter and 20 mm height is cut by wire cutting process from the cross section of failed helical suspension spring as shown in Fig. 14. This cut specimen is polished and etched with 3% nital solution. The prepared specimen to see microstructure is shown in Fig. 15.

The microstructure of the specimen is captured at 100X (Fig. 16). It shows transverse cracks running across the cross section of the wire. Also, formation of bainite and martensite was observed which results in difference between surface hardness and core hardness.

5.5 Stress Evaluation

A cubical hole of dimension $0.5 \times 0.5 \times 0.5$ mm³ was generated on the outer periphery of the spring wire in the CAD model of spring forming coil mechanism in order to bring surface wear on the spring coil surface as shown in Fig. 17 [4]. Static analysis of this CAD model has been performed on ANSYS® software. The computational analysis results revealed a high stress concentration zone near the

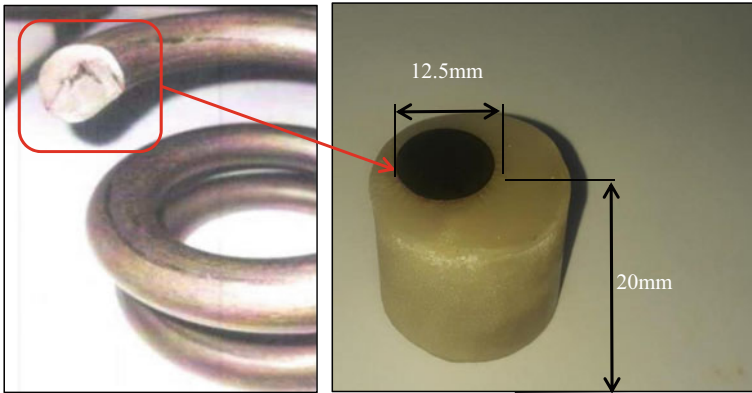


Fig. 14 Specimen cut from the cross section of failed helical suspension spring

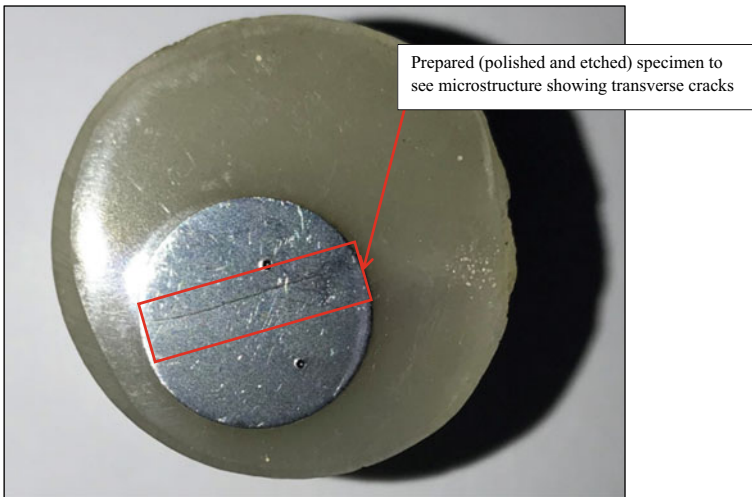


Fig. 15 Prepared (polished and etched) specimen to see microstructure

cubical hole (Fig. 18). It is found that the maximum equivalent (Von-Mises) stress of spring coil is 1721.5 MPa (Fig. 19), which is more than 1704 MPa, i.e. ultimate tensile strength of spring material SAE-9254, hence spring coil is broken/failed at this point.

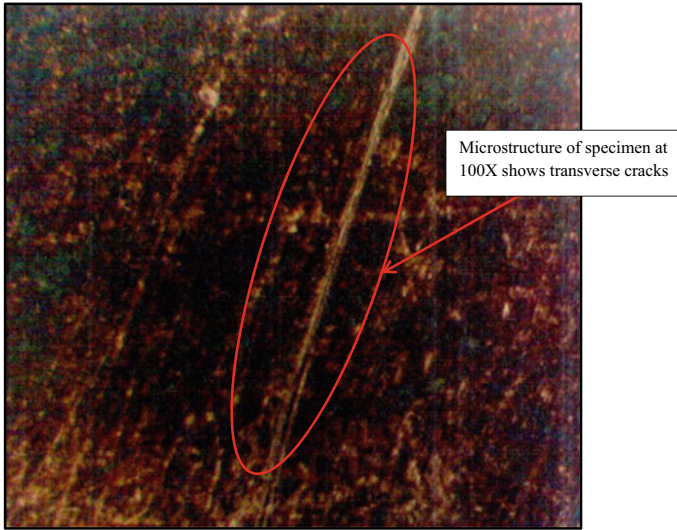


Fig. 16 Microstructure of specimen at 100X shows transverse cracks

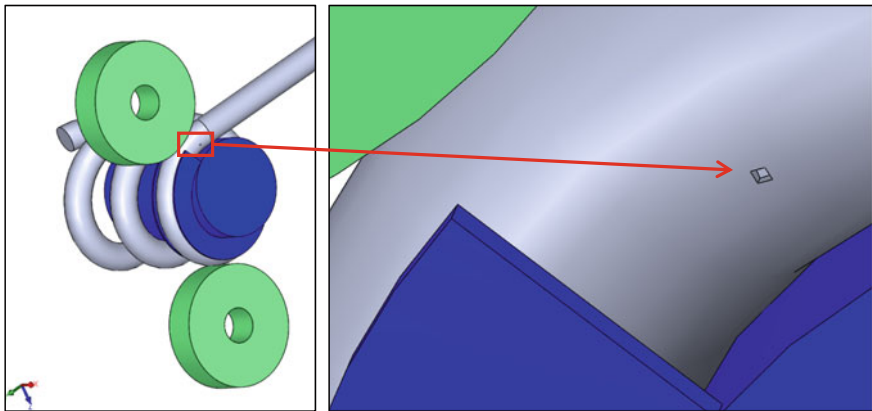


Fig. 17 Cubical hole on the outer surface of spring wire

6 Conclusion

Various research work has been done on different types of suspension spring material and were mainly focussed on service-based failure. But the research work is limited on this particular spring steel material, i.e. SAE-9254. In this research work, we have investigated a prematurely failed SAE-9254 helical suspension spring which was failed during its manufacturing stage. A discussion on different types of premature failure has been discussed in the literature review. We proposed representation in both

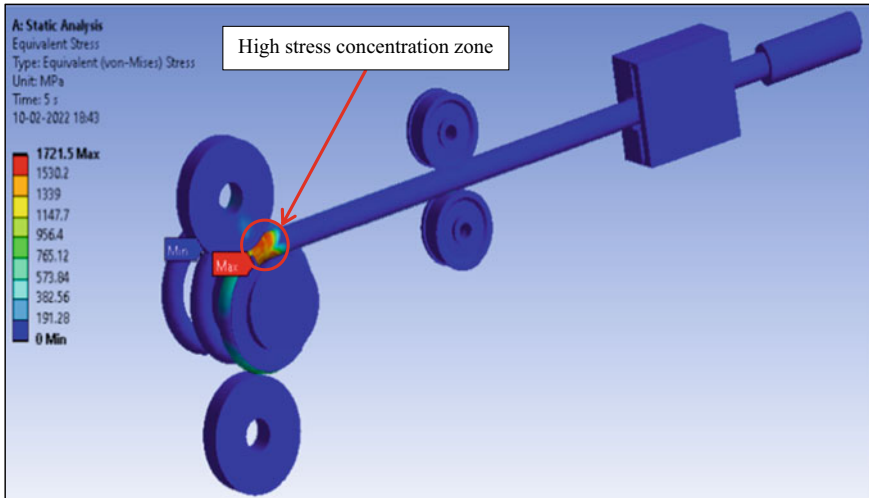


Fig. 18 High stress concentration zone

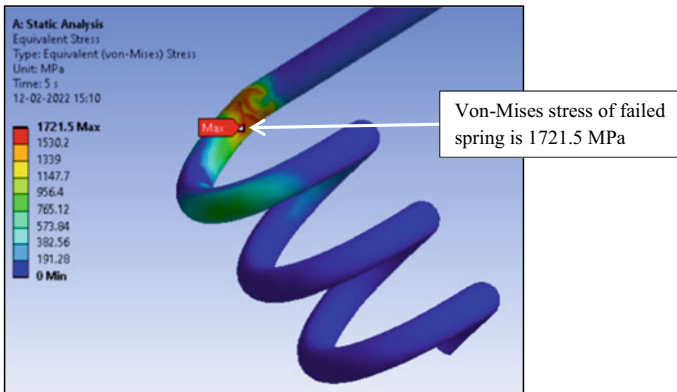


Fig. 19 Von-Mises stress of failed spring

experimental and computational aspects. First, a helical spring of SAE-9254 material has been designed to find different parameters and then an experimental investigation has been carried out to find the root causes of its failure, and finally, a computational analysis has been performed to validate the results. Following conclusions have been made from the results obtained from experimental and computational analysis.

- Through experimental results, it is concluded that the spring has been failed due to the formation of a transverse crack on its cross section. These cracks are initiated at the pits which created regions of high-stress concentration and propagated further on loading, Further, decarburization, skin hardness and formation of bainite and

martensite are responsible factors to bring the differences in surface and core hardness and catastrophic failure of spring.

- From the computational results, it is observed that at the point of surface wear there is a high-stress concentration zone. At this zone, Von-Mises stress is evaluated as 1721.5 MPa which is higher than the ultimate tensile strength of high strength spring steel SAE-9254, i.e. 1704 MPa, and hence, the spring coil is broken/failed at the point of surface wear.

References

1. Sataynarayana K, Tamada U, Gowri B, Sai D, Ganesh A, Bharath K, Narayana KS (2020) Design and static analysis on a helical spring for two wheeler. *JAC J Compos Theory* 13:1439–1449
2. Berti G, Monti M (2010) FEM analysis of the forming process of automotive suspension springs. Semantic Scholar
3. Ke J, Wu Z, Liu Y, Xiang Z, Hu X (2020) Design method, performance investigation and manufacturing process of composite helical springs: a review. *Compos Struct* 252:112747. <https://doi.org/10.1016/j.compstruct.2020.112747>
4. Prawoto Y, Ikeda M, Manville S, Nishikawa A (2008) Design and failure modes of automotive suspension springs. *Eng Fail Anal* 15(8):1155–1174. <https://doi.org/10.1016/j.engfailanal.2007.11.003>
5. Ikpe AE, Owunna I (2017) Design of vehicle compression springs for optimum performance in their service condition. *Int J Eng Res Afr* 33:22–34. <https://doi.org/10.4028/www.scientific.net/jera.33.22>
6. Das S, Talukdar S, Solanki V (2020) Breakage of spring steel during manufacturing: a metallurgical investigation. *J Fail Anal Prev* 20:1462–1469. <https://doi.org/10.1007/s11668-020-00993-9>
7. Fragoudakis R, Karditsas S, Savaidis G, Michailidis N (2014) The effect of heat and surface treatment on the fatigue behaviour of 56sic7 spring steel. *Procedia Eng* 74:309–312. <https://doi.org/10.1016/j.proeng.2014.06.268>
8. Puff R, Barbieri R (2014) Effect of non-metallic inclusions on the fatigue strength of helical spring wire. *Eng Fail Anal* 44:441–454. <https://doi.org/10.1016/j.engfailanal.2014.05.013>
9. Suzuki T, Ono Y, Miyamoto G, Furuhashi T (2010) Effects of Si and Cr on bainite microstructure of medium carbon steels. *ISIJ Int* 50:1476–1482. <https://doi.org/10.2355/isijinternational.50.1476>
10. Gonzalez MPV, Maria G-M, Muro AP (2019) Study of a torsion spring fracture. *Eng Fail Anal* 98:150–155. <https://doi.org/10.1016/j.engfailanal.2019.01.075>
11. Pastorcic D, Vukelic G, Bozic Z (2019) Coil spring failure and fatigue analysis. *Eng Fail Anal* 99:310–318. <https://doi.org/10.1016/j.engfailanal.2019.02.017>
12. Vukelic G, Brcic M (2016) Failure analysis of a motor vehicle coil spring. *Procedia Struct Integrity* 2:2944–2950. <https://doi.org/10.1016/j.prostr.2016.06.368>
13. Das SK, Mukhopadhyay NK, Kumar BR, Bhattacharya DK (2007) Failure analysis of a passenger car coil spring. *Eng Fail Anal* 14(1):158–163. <https://doi.org/10.1016/j.engfailanal.2005.11.012>
14. Sreenivasan M, Kumar MD, Krishna R, Mohanraj T, Suresh G, Kumar H, Charan AS (2020) Finite element analysis of coil spring of a motorcycle suspension system using different fibre materials. *Mater Today Proc* 33(1):275–279. <https://doi.org/10.1016/j.matpr.2020.04.051>
15. Yan S, Wang Q, Chen X, Zhang C, Cui G (2019) Failure analysis of an automobile coil spring in high-stress state. *J Fail Anal Prev* 19(2):361–368. <https://doi.org/10.1007/s11668-019-00607-z>

16. Stephen C, Selvam R, Suranjan S (2019) A comparative study of steel and composite helical springs using finite element analysis. Adv Sci Eng Technol Int Conf (ASET). <https://doi.org/10.1109/ICASET.2019.8714314>